
B. Wittekoek
Deltares, Delft
Netherlands


S.J.M. van Eekelen
Deltares, Delft
Netherlands


A. Bezuijen
Deltares, Delft
Netherlands


J. Terwindt
Data Engineer at Scarp
DENA, Sweden


O. Detert
Huesker Synthetic
Germany


J.H. van den Berg
Huesker Synthetic
Germany


D. König
Ruhr-Universität Bochum
Germany

GEOGRID-ANCHORED SHEET PILE WALLS UNDER STRIP FOOTING SURCHARGE LOADING, SMALL-SCALE EXPERIMENTS

Introduction

A geogrid-anchored sheet pile wall (SPW) is a relative new application of geogrids (van Duijnen et al., 2022, Wittekoek, 2020, Wittekoek et al., 2022). The system is closely linked to a retaining wall of reinforced soil with a full-height facing as well as to a traditional anchored SPW. However, the geogrid-anchored SPW has more embedment than a retaining wall of reinforced soil. And contrary to a traditionally anchored SPW, a geogrid anchor is also effective within the active soil wedge when the SPW deforms. This paper looks at small scale experiments, to get a feeling for how the system works. This paper is a shorter version of Wittekoek et al. (2023).

Small-scale experiments

Figure 1 shows the test set-up of the small-scale experiments. The aluminium model-SPW models the upper part of the embedded part of the SPW and was free to slide along the box bottom. The polypropylene (PP) model-geogrid had a short-term stiffness of 191 kN/m at 2% axial strain and a short-term tensile strength of 16.2 kN/m at a maximum strain of 13.5%. Table 1 lists the properties of the sand fill.

A silicon block model at the passive side has a stiffness of 159 kPa up to a strain of at least 8%. This silicon block was tailored to simulate passive resistance as realistic as possible. The strip surcharge load is applied by loading a 0.1 m wide footing with a barrel that is filled with water during the test (the blue barrel in Figure 1). The soil-wall friction was minimized with a lubricated thin (< 1mm) transparent silicone sheet. Wittekoek et al. (2022) showed that tests in an eight times wider test box gave similar slip surfaces, proving that the narrow box results were sufficiently reliable to analyse qualitatively. The movement of the soil was tracked using the Particle Image Velocimetry (PIV) technique as implemented by Stanier et al. (2015).

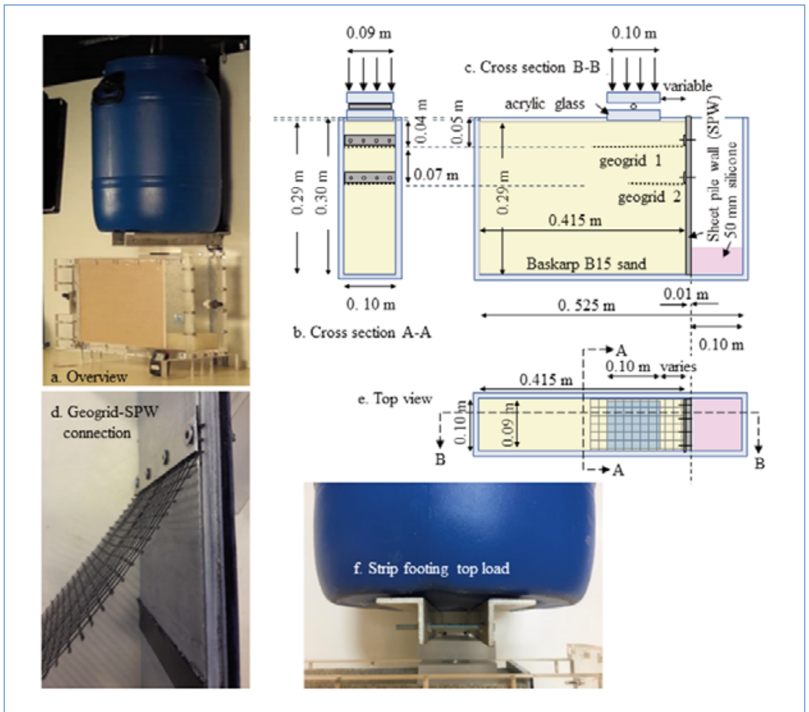

Figure 1 – Test set-up.

Results small-scale experiments

THE LOCATION OF THE STRIP SURCHARGE LOAD

Figure 2 shows how the location of the surcharge load determines the failure mechanism. Two slip surfaces develop from the two edges of the strip footing towards the SPW, dividing the soil into three different zones. Zone I is characterized by rigid soil body motions. The active zone II slides along the critical slip surface 1A. Zone III is stable. The third slip surface in Figure 2 only occurred in Test 19, not in duplicate Test 18 or any other test.

A greater distance between load and SPW results in stiffer behaviour (Figure 3): the wider slip surfaces mobilize more shear resistance, and the load is distributed to deeper soil. Figure 3a and b differ remarkably. If the load is at 84 mm from the SPW, the 60 mm geogrid is located fully in zone I. Nevertheless, the bearing capacity increases compared to the situation without geogrid. The load position has less influence for longer geogrids (Figure 3c and d).

GEOGRID ANCHOR LENGTH

Longer geogrids provide more resistance (Figure 4) which increases the bearing capacity of the entire system. The longest geogrid initially behaves stiffer than the shorter geogrids. Figure

Table 1 – Properties Baskarp B15 sand.

Parameter	*Value*	*Parameter*	*Value*
Relative density I_D (%)	63-83	Dilatancy angle ψ^{triax} (°)	15.0
Median particle diameter D_{50} (mm)	0.137	Cohesion *c* (kPa)	0.6
Coefficient of uniformity D_{60}/D_{10} (-)	1.6	Secant Young's modulus at confining pressure of 100 E_{50}^{ref} (MPa)	72.4
Secant internal friction angle φ_{sec}^{triax} (°)	37*	Power in power law material stiffness *m* (-)	0.54
Residual internal friction angle φ_{res}^{triax} (°)	34	Poisson ratio ν (-)	0.25

* Plane strain value of ($^{11}/_{9}$ • triaxial value =) 45°.

ABSTRACT

Small-scale experiments on geogrid-anchored sheet pile walls (SPWs) under strip footing surcharge loading were conducted at the Deltares laboratory. The following was concluded from the experiments. Two slip surfaces develop, starting at the edges of the strip footing. They divide the soil behind the SPW into three zones. The paper analyses the contributions of each of these zones to the failure load of the structure. The location of the strip footing surcharge load, the geogrid length and the number of geogrid anchors all affect the failure load of the structure. Furthermore, the slip surface reorients at the intersection with geogrids, and even very short geogrid anchors contribute to the total resistance.

Table 2 – The test series. This paper gives results of the tests with bold-printed numbers. Duplicate tests are denoted by a forward slash.

Test number	12/13	14/15	16/17/45	18/19	20/21	22/23	28	30	31	41/42	43/44	47	48	51	52
Number of geogrids	1	1	1	1	2	2	1	1	1	1	1	0	0	1	1
Length geogrids (mm)	110	110	180	180	180+110	180+110	60	60	60	180	110	-	-	130	130
Connected to SPW?	Yes	Yes	Yes	Yes	Yes	Yes	Yes	Yes	No	No	No	-	-	No	Yes
Vertical distance top SPW-geogrid (mm)	50	50	50	50	50+120	50+120	50	50	50	50	50	-	-	50	50
Horizontal distance surcharge load-SPW (mm)	30	60	30	130	130	30	30	84	30	30	30	84	30	30	30
Relative density fill (%)	67/71	73/74	68/74/76	74/73	71/64	74/78	81	78	68	75/76	69/76	75	71	67	65

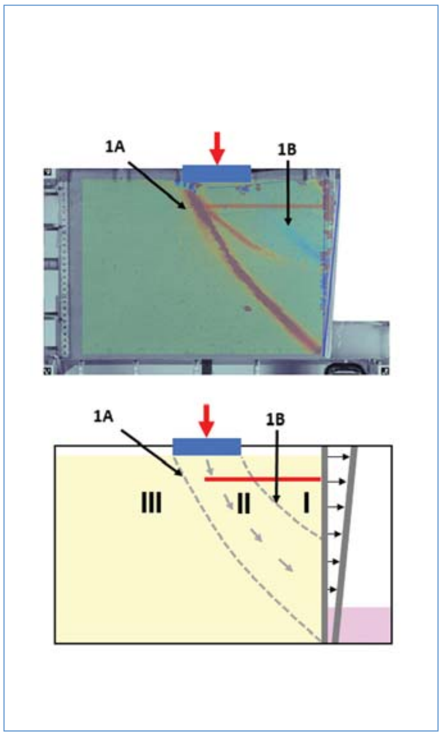

Figure 2 – Slip surfaces for a surcharge load of ~4 kN/m. Test 19. 1A: critical slip surface and 1B: secondary slip surface. The slip surfaces divide the soil in three zones: active zone II between zones I and III.

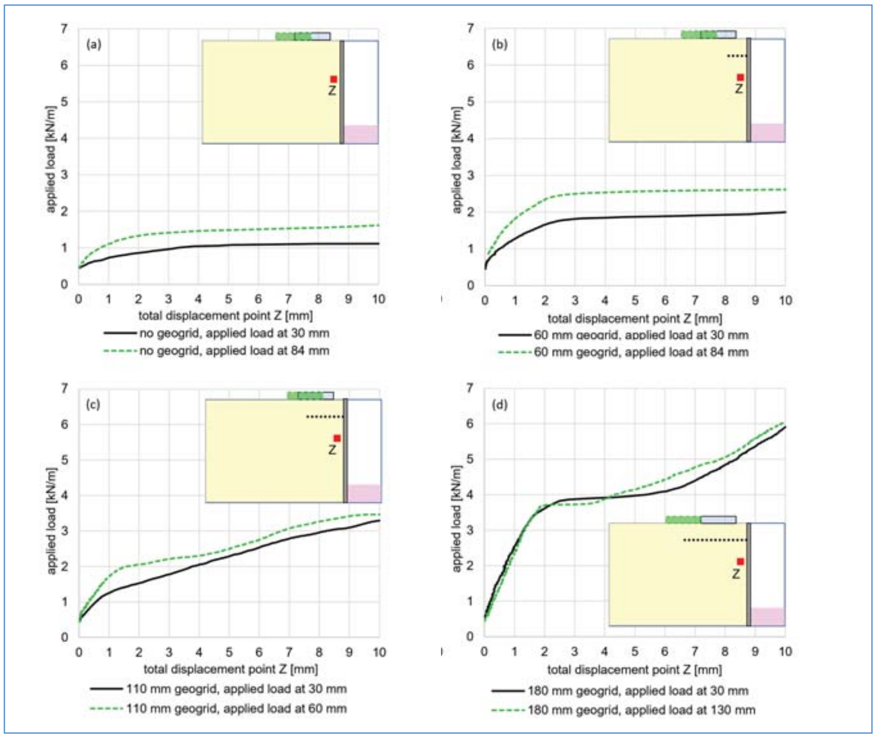

Figure 3 – Influence of the location of the surcharge load (a) without geogrid (b) 60 mm geogrid (c) 110 mm geogrid and (d) 180 mm geogrid.

4b shows a straight slip surface for all geogrids. Only for the longest geogrid of 180 mm (Test 45), the slip surface crosses the geogrid and a second curved slip surface develops. The initial straight slip surface is therefore not the critical one. The geogrid is activated more efficiently, and the orientation of the slip surface at the intersection with the geogrid changes. The geogrid is activated more efficiently, and the orientation of the slip surface at the intersection with the geogrid changes, like also found by Ziegler (2010). The slip surface therefore becomes longer and curved.

A SECOND GEOGRID ANCHOR

Figure 5 compares 1 and 2 geogrids. The deformations are equal up to a surcharge load of 3.0 kN/m. Above 4.0 kN/m, the SPW slides along the box bottom in both tests. This failure mode is triggered by the relatively high resistance of the geogrid anchor(s). For this higher surcharge load, the second geogrid limits the deformations when the vertical pressure on the geogrids (and therefore the soil-geogrid interface friction) increase. This is in line with the 2D FEM calculations of Schoen et al. (2023), that showed that the geogrid anchor is more effective when installed at a lower level.

Contrary to expectations, point Z settles more than point Y. The second geogrid increases this difference. Obviously, the geogrids limit the settlement of the soil above. Figure 6 shows how the second geogrid changes the slip surface: it becomes slightly wider, and therefore longer, as it circumvents the second geogrid.

CONNECTION GEOGRID – SHEET PILE WALL

In four tests, the geogrid was not connected to the SPW (Figure 7). From these tests we conclude that:

- Connecting the geogrid increases the failure load.
- Short non-connected geogrids ≤ 130 mm hardly contribute to the failure load.
- Short connected geogrids ≤ 130 mm increase the failure load, although they are located in zones I and II only. So, zones I and II are only activated when the geogrid is connected to

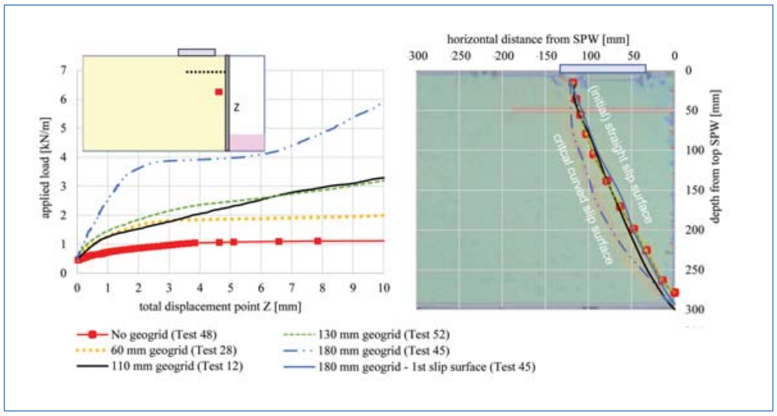

Figure 4 – Influence of the geogrid length. Surcharge load at 30 mm from the SPW. The background of the right-hand figure is Test 45 (180 mm geogrid).

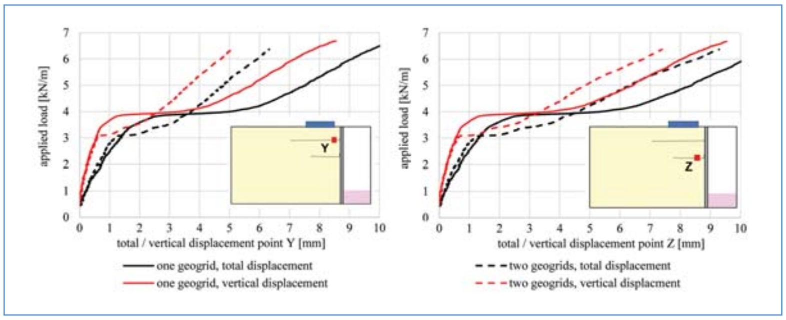

Figure 5 – Load-displacement behaviour for 1 or 2 geogrids. Surcharge load at 30 mm from the SPW. Tests 45 and 22: both have a 180 mm geogrid at the same position, Test 22 has a second geogrid (110 mm).

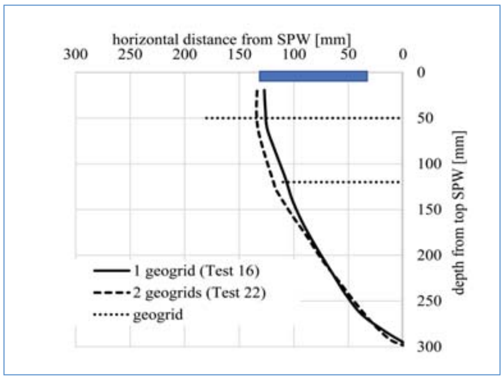

Figure 6 – Slip planes for 1 or 2 geogrids.

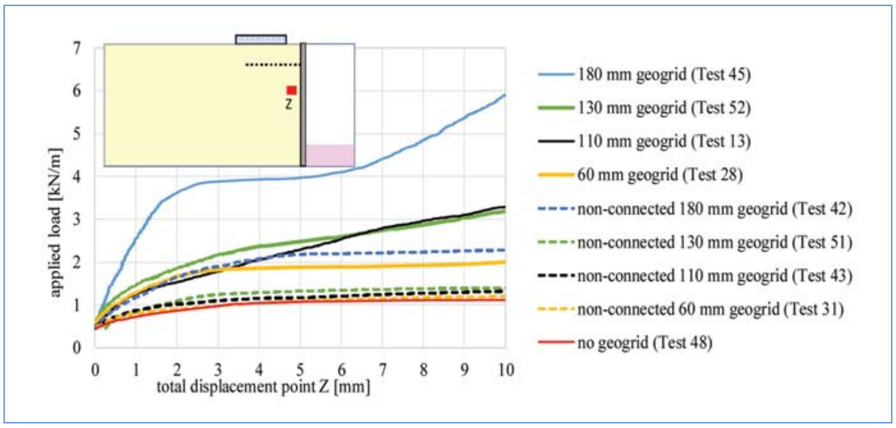

Figure 7 – Difference between geogrids that are connected or not to the SPW.

the SPW and the geogrid has moved downwards with the soil in zone II.

- Short geogrids ≤130 mm do not reinforce the soil, because the short non-connected geogrids do not provide more failure resistance than found in the situation without geogrid.
- The increase in failure load due to connecting the geogrids (≤130 mm) indicates the presence of the 'membrane effect'. This term refers to the capacity of the geogrid to be deformed, while absorbing forces that were initially perpendicular to its surface. When the geogrid moves downwards with the soil in Zone II, tensile forces develop in the geogrid through which the geogrid transfers vertical soil pressures to zone I, the SPW, if connected, and zone III.
- The 180 mm geogrid, even if not connected to the SPW, contributes to the total resistance. The failure load results from the pull-out resistance in zones I and III.
- Connecting the 180 mm geogrid activates the rear part of the geogrid (zone III) more effectively and increases the failure load. However, the rear part contributes most to the total resistance at higher load levels while the geogrid is being pulled out by the sliding soil mass in zone II.
- The total resistance of a connected geogrid anchor consists of contributions of the membrane effect (zone I), frictional resistance (zone II) and pull-out resistance (zone III).

Conclusions

A series of small-scale tests of geogrid-anchored SPWs led to the following conclusions. Two slip surfaces, starting at the edges of the strip footing, divide the fill behind the SPW into three zones: the active zone II, zone I between SPW and active zone II. The paper analyses the contributions of each of these zones to failure. The location of the strip footing surcharge load, the length of the geogrids and the number of geogrid anchors affect the failure load of the structure. The slip surface at the intersection of the critical slip surface reorients with the geogrids, and even a very short geogrid anchor contributes to the total resistance.

Acknowledgements

The authors are grateful for the support of the TKI-PPS funding of the Dutch Ministry of Economic Affairs, Deltares, Delft University of Technology, GeoTec Solutions, Huesker BV, Huesker GmbH and Ruhr-Universität Bochum Germany.

References

- Schoen, M., König, D., Lavasan, A.A., Wichtmann, T., Hölter, R., Wittekoek, B., van Eekelen, S.J.M., van Duijnen, P.G. & Detert, O. 2023. Numerical investigation of geogrid back-anchored sheet pile walls. In: proc. 12 ICG, Rome, Italy.
- Stanier, S.A., Blaber, J., Take, W.A. and White, D.J. (2015). Improved image-based deformation measurement for geotechnical applications. Canadian Geotechnical Journal. https://doi.org/ 10.1139/cgj-2015-0253
- van Duijnen, P.G., Detert, O., Lavasan, A.A., van den Berg, J., König, D., Hölger, R., van Eekelen, S.J.M. 2022. Geogrid-anchored sheet pile walls: first trial project. In: proc. Eurogeo7, Warsaw, Poland.
- Wittekoek, B. 2020. Analysis of the behaviour of geogrid-anchored sheet pile walls. Small-scale experiments and 2D Plaxis analysis. MSc thesis TU Delft. https://repository.tudelft.nl/islandora/object/uuid%3A94cf64cc-ff09-4fbe-bde8-42d914 b3c7d0.
- Wittekoek, B., van Eekelen, S.J.M., Terwindt, J., Korff, M., van Duijnen, P.G., Detert, O. and Bezuijen, A. 2022. Geogrid-anchored sheet pile walls; a small-scale experimental and numerical study. Geosynthetics International. https://doi.org/10.1680/jgein.22.00501
- Wittekoek, B., van Eekelen, S.J.M., Bezuijen, A., Terwindt, J., van Duijnen, P.G., Detert, O., van den Berg, J.H., and König, D., 2023. Geogrid-anchored sheet pile walls under strip footing surcharge loading, small-scale experiments. In: proc. 12ICG, Rome, Italy.
- Ziegler, M. 2010. Investigation of the Confining Effect of Geogrid Reinforced Soil with Plane Strain Model Wall Tests. Aachen, Germany: Rheinische Westfälische Technische Hochschule Aachen (RWTH).